Four Dimensional Localisation With Motivic Neutrinos

M. D. Sheppeard
Aranui, Christchurch 8061, New Zealand
E-mail: marnisheppeard@gmail.com

Abstract. Quantum gravity traditionally begins with path integrals for four dimensional spacetimes, where the subtlety is in smooth structures. From a motivic perspective, the same diagrams belong to ribbon categories for quantum computation, based on algebraic number fields. Here we investigate this divide using the principle of the neutrino CMB correspondence, which introduces a mirror pair of ribbon diagrams for each Standard Model state. Categorical condensation for gapped boundary systems in extended quantum double models extends the modular structure to encompass Kirby diagrams.

Keywords: algebraic integers, gapped boundary, modular tensor, motivic, neutrino

1. Introduction

In motivic gravity we study the localisation to four dimensions from a categorical perspective, which is radically different from the traditional one. From this viewpoint [1][2], physical axioms become increasingly complex, beyond the knot and ribbon categories [3][4][5] in dimension 3, which underlie topological quantum computation for anyon and gapped boundary systems [6][7][8][9][10]. We permit additional time directions, since every string in a quantum circuit is permitted to twist in its time domain, prior to the consideration of a global spacetime. In six dimensions, three times for mass generation are localised to a single time coordinate by the neutrino CMB correspondence [11][12], which associates one right handed neutrino mass to the present day CMB temperature. This thermal gravity is potentially evidenced by experiments on the topological thermal Hall effect [13][14].

In the gauge theory setting, the Jones polynomial appears [15] with Wilson loops for the Chern-Simons action. Inspired by a holographic principle for a computational mirror, or Majorana holography [16], we study Witten's tower of dimensions [17][18] using categorical algebra and number theory. The Jones invariant [19] is interpreted [17] in 4D using electric magnetic duality, and this is extended to 5D with categorification for Khovanov homology [20][21].

Electric magnetic duality is associated to the dyonic structure of ribbon particle states, which appear as mirror pairs. In the basic scheme, B_3 diagrams in S^3 acquire a $U(1)$ ribbon twist to give an $SU(2) \times U(1)$ compactified Minkowski space as an emergent feature of discrete $SU(2)$ braid group representations. Since the gauge groups determine the spacetime, a complexification of the Chern-Simons action immediately suggests a six dimensional setting. Motivic gravity starts here [2] with two copies of CSFT: one for QCD and one for the IR scale of neutrino mass [22][23].

Topology change is morally a topos theoretic concept [24]. Exotic structures on 4-manifolds are defined by the integral form and associated knot and link diagrams [25]. In quantum topos theory, real analysis is not a good starting point for emergent geometries in low dimensions, and one expects the axioms to merge algebraic number theory and combinatorics, just as Feynman amplitudes are evaluated in a ring of periods rather than $\mathbb{C}$. The appendix shows how algebraic number theory is linked to basic observables in quantum mechanics. We insist that observables dictate algebra, in order to minimise the analytical baggage that must be carried around, and analysis should be re-axiomatised in quantum logic.

The associahedron [26][27] polytope is an axiom for an n-category. In this paper we explain how the associahedra are closely related to knots. The connection between instanton moduli and knots is studied using fermion condensates [28], both for (supersymmetric) QCD and an IR counterpart, which we attribute to neutrino gravity [2]. Knots are extended to ribbons, which are the building blocks of template diagrams. All diagrams are interpreted category theoretically, focusing on Fibonacci anyon categories and condensation algebras [29], which we relate to the Kirby calculus.

Section 2 introduces the golden rings, integral forms and electric charges. In section 3 we put electric magnetic duality in a motivic framework, review the Koide rest mass phenomenology, and list the fundamental states of the Standard Model. Section 4 discusses categorical algebras and polytopes, and section 5 concludes with comments on motivic integration. The essential claim is that mass generation in gapped boundary systems has an abstract analog under the neutrino CMB ansatz, which is the true origin of inertial mass in quantum gravity. Here we do not discuss Yang-Mills doubles, entanglement measures, black holes or AdS geometries, although obvious connections exist.

2. Towards 4-manifolds

2.1. The golden ring and Fibonacci categories

Experimental precision does not actually require $\mathbb{R}$ or $\mathbb{C}$, except in axiomatic questions of computability. Like the adeles, where $\mathbb{R}$ appears as the infinite prime, we imagine real manifolds emerging in infinite dimensional computations, whereas a qudit state space makes do with algebraic numbers, canonically selected by the quantum mechanical question.

Consider the various triangles in the pentagram of the appendix. The little blue triangle below the bisected top spike of the pentagram is equivalent to the top blue right angled triangle, with an angle of $18^\circ = \tan^{-1}(\phi\rho)^{-1}$, with $\phi = (1+\sqrt{5})/2$ the golden ratio and $\rho = \sqrt{\phi+2}$ the diagonal of the golden rectangle. The little 18° bisects the 36° at the red chord, which is a piece of a smaller red pentagon, initiating a discrete zoom-in quasilattice of pentagonal coordinates for the plane. In [30] it is shown that the 8 dimensional rational half integers $\mathbb{Z}^8/2$ may be embedded in $\mathbb{C}$ using the *golden ring* $\mathbb{Z}[\rho]$ (see the appendix). One basis of $\mathbb{R} \subset \mathbb{C}$ is given by

$$x = x_0 + x_1\phi + x_2\rho + x_3\phi\rho \tag{1}$$

for integral x_i. Eight dimensions, in the form $x + iy$, is an obvious setting for the $\mathbf{e_8}$ lattice and its intersection form.

There are four types [31] of Fibonacci ribbon category that use golden geometry: two based on minimal models and two for the affine chiral algebras $G_{2,1}$ and $F_{4,1}$. Note that $G_{2,1} \times F_{4,1} \subset E_{8,1}$. The affine VOAs correspond to a central charge

$$c = \frac{k\,\dim(\mathbf{g})}{k + h^\vee} \tag{2}$$

at level k, and in general the deformation parameter u is given by

$$u^{-1} = e^{\pi i c/2}. \tag{3}$$

For $\phi(u^2+1) = -u$, we have the usual Fibonacci objects I and X with the quantum dimension of X equal to ϕ. The Yang-Lee model at the tenth root $u = e^{\pi i/5}$ is the representations of the model $M(2,5)$ with $c = -22/5$. In the modular categories, for a unitary VOA, the ribbon twist is given by the conformal weight. The modular matrices here take the form

$$S = \rho^{-1} \begin{pmatrix} 1 & \phi \\ \phi & -1 \end{pmatrix}, \quad T = u^{1/6} \begin{pmatrix} 1 & 0 \\ 0 & u^2 \end{pmatrix}. \tag{4}$$

For $G_{2,1}$ at $u = e^{3\pi i/5}$ the phase $u^{1/6}$ in T is still golden, and similarly for $F_{4,1}$.

If we wanted a basic deformation of $\omega = (-1+\sqrt{-3})/2$ for the Eisenstein integers, we would require $c = 6$, which appears in a $(4,4)$ superconformal theory for Mathieu moonshine.

We do not use gauge theory to evaluate knot invariants. The Jones or HOMFLYPT polynomials are evaluated using skein relations, and the Khovanov complex is defined as usual using smoothings. Since our link strands are not geometric in the classical sense, what matters is the information content, or complexity, of a diagram.

2.2. The role of $\mathbf{e_8}$

A 4-manifold is characterised by its integral form [25], and a key component in the classification of integral forms is the $\mathbf{e_8}$ form

$$E_8 = \begin{pmatrix} 2 & 1 & 0 & 0 & 0 & 0 & 0 & 0 \\ 1 & 2 & 1 & 0 & 0 & 0 & 0 & 0 \\ 0 & 1 & 2 & 1 & 0 & 0 & 0 & 0 \\ 0 & 0 & 1 & 2 & 1 & 0 & 0 & 0 \\ 0 & 0 & 0 & 1 & 2 & 1 & 0 & 1 \\ 0 & 0 & 0 & 0 & 1 & 2 & 1 & 0 \\ 0 & 0 & 0 & 0 & 0 & 1 & 2 & 0 \\ 0 & 0 & 0 & 0 & 1 & 0 & 0 & 2 \end{pmatrix}. \tag{5}$$

But an $\mathbf{e_8}$ manifold cannot be smooth because the form does not diagonalise over the rational integers. It does, however, diagonalise [32] over the golden integers $\mathbb{Z}[\phi]$, where $\phi = (1+\sqrt{5})/2$ is the golden ratio. As is well known, E_8 is positive definite, even and unimodular for closed manifolds. Let $\sigma(Q)$ be the signature of the form Q and $r(Q)$ its rank. All such quadratic forms take the form [25]

$$Q = \frac{\sigma(Q)}{8} E_8 \oplus \frac{r(Q) - |\sigma(Q)|}{2} \begin{pmatrix} 0 & 1 \\ 1 & 0 \end{pmatrix}, \tag{6}$$

where the 2×2 factors are forms for either the torus T^2 (for $H_1(T^2, \mathbb{Z}_2)$) or $S^2 \times S^2$ in dimension 4. This ambiguity will matter later on. One important smooth space, which contains a topological component that cannot be smoothed, is the Kummer (or K3) surface, with its 22 dimensional form

$$Q_{K3} = E_8 \oplus E_8 \oplus \begin{pmatrix} 0 & 1 \\ 1 & 0 \end{pmatrix} \oplus \begin{pmatrix} 0 & 1 \\ 1 & 0 \end{pmatrix} \oplus \begin{pmatrix} 0 & 1 \\ 1 & 0 \end{pmatrix}. \tag{7}$$

The construction uses a connected sum of three copies of the 4-manifold $S^2 \times S^2$, corresponding to the triple of σ_X flip matrices. A quotient of this sum by a certain embedding, related to the Kummer surface, yields a fake version of $\mathbb{R}^4$, wherein a theorem of Freedman [33] characterises good copies of $\mathbb{R}^4$ by the conditions: simply connected, non-compact, without boundary, $H_2(M, \mathbb{Z}) = 0$, homeomorphic to $S^3 \times [0, \infty)$. It turns out that there are an uncountable number of inequivalent smooth structures on $\mathbb{R}^4$, and this complexity is unique to dimension 4 due to surface knotting.

The elliptic genus for the K3 surface [34] is

$$Z_{K3}(\tau,z)=8[(\frac{\theta_2(\tau,z)}{\theta_2(\tau,0)})^2+(\frac{\theta_3(\tau,z)}{\theta_3(\tau,0)})^2+(\frac{\theta_4(\tau,z)}{\theta_4(\tau,0)})^2], \tag{8}$$

for $\theta_i(\tau,z)$ the Jacobi theta functions. Nowadays it is written in terms of dimensions of irreducible representations [35] for the Mathieu group M_{24}, in Mathieu moonshine [36] and its umbral generalisation [37]. Moonshine for the Monster group uses the j-invariant, which is analogously defined by

$$j(q)=32\frac{(\theta_2(0,q)^8+\theta_3(0,q)^8+\theta_4(0,q)^8)^3}{(\theta_2(0,q)\theta_3(0,q)\theta_4(0,q))^8}. \tag{9}$$

The associated Eisenstein series E_4 counts vectors in the shells of the $\mathbf{e_8}$ root lattice. The lattices underlying modular forms are fundamental. Whenever we see a triplet of terms, as in (9), we think of some form of triality. In the Jordan algebra $J_3(\mathbb{O})$, triality acts on the three off-diagonal copies of $\mathbb{O}$, and this extends to generalised 3×3 algebras for ribbon categories.

How about the physics? As in table 1, the exact gauge symmetries $U(1)_Q$ and color $SU(3)_C$ are directly associated, respectively, to ribbon twists and a triplet of ribbon strands, so that the 8 negative electric charges for $\{\nu,e^-,d,\overline{u}\}$ lie on the vertices of a 3-cube [38][39], whose directions label ribbon strands. Such a 3-cube, in figure 1, determines a basis for the octonions $\mathbb{O}$. Complexification brings in antiparticles, for a total 4-cube of charges, and complex conjugation is charge conjugation in the $\mathbb{C}\otimes\mathbb{O}$ ideal algebra, which extends to crossing flips in the ribbon picture. A 7-cube introduces magnetic data with 7-stranded ribbon diagrams, and in general the extended M theory dimension equals twice the number of ribbon strands.

Electroweak symmetries are broken back-to-front: the Higgs mass emerges from the inverse see-saw rule [2], which pairs the Planck scale and IR neutrino mass scale at 0.01 eV. There is no need to introduce further local states beyond the SM, because the new RH neutrino is associated to a cosmological scale.

2.3. The Kirby calculus and electric charge

An axiomatic approach to invariants constructs state sums from categorical data. Barrett et al [40] consider a functor from a spherical fusion category into a ribbon fusion category for the 2-handlebody of the 4-manifold, in order to define smooth invariants by weakening the sliding law in a ribbon category. A 4-manifold is determined up to diffeomorphism by its 2-handlebody attachments, where a 2-handle piece is essentially a framed knot in the S^3 boundary of the 0-handle.

For a 2-handle in 4 dimensions, the framing classes are characterised by $\pi_1(O(2))=\mathbb{Z}$ [25], whereas in 3 dimensions the only framings are 1 or $\theta^{1/2}$, where θ represents a full ribbon twist. This distinction is crucial here, because quantised electric charge is given by ribbon twists. Three dimensions only permits two charges, whereas physics requires three values $0,\pm 1$. Often we denote these charges [1] by the cubed roots of unity 1, ω and $\overline{\omega}$, when θ behaves like a phase. To obtain this $\mathbb{Z}_3$ we have to go to four dimensions, and quotient out by the natural $3\mathbb{Z}$: a triple of half twists $\theta^{3/2}$ equals -1 under the cubed root representation, while $B_2=\mathbb{Z}$ represents -1 by a single half twist. In other words, electric charge appears with the holographic extension of $2+1$ dimensions through the Kirby interpretation of diagrams.

A Kirby diagram [41] of knots and balls accounts for all the attachments in $\mathbb{R}^3$ for a 4-manifold (there are really no real numbers; just diagrams). A single knot in the Kirby diagram will cancel a 1-handle (two balls in $\mathbb{R}^3$) if it has ends attached to each S^2 boundary. In an Akbulut diagram, the balls of a 1-handle are replaced by marked circles, so that the entire 4-manifold is specified

by a diagram for a ribbon fusion category [5]. Let us stress, we wish to replace the $S^2 \cup S^2$ by $S^1 \cup S^1$, introducing gapped boundary structures.

To start with, we consider modular ribbon categories, which have a finite number of isomorphism classes of simple objects, and an invertible matrix s_{ij} defined by Hopf links on the objects i and j. Kirby framed link diagrams are associated to ribbon vertices, and we see how simple ribbon pictures may give rise to complicated links.

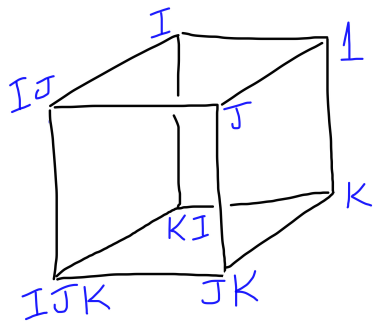

Figure 1. Octonion units on a cube

3. Knots and gravity

3.1. Electric magnetic duality

Categorical axioms lie at the foundation of both condensed matter physics and computer science. It turns out that topological insulators, for instance, are a good intuition for the dyonic mirror [42] that defines holography in the ribbon particle scheme. Every diagram is interpreted categorically, so that a cube exists in the same sense as an associahedron, which is an axiom for an n-category. On the one hand we have polytopes, and dually we have generalised string diagrams. This emphasis is different from 4-categories for geometric quantisation based on symmetry [43], but we still have to consider arrows in dimensions 0 and 1, which are trivial for a braided monoidal category. The idea is to associate geometric duality to cohomological duality, where the mirror ribbon category occupies the dual dimensions.

The electric charges of the (massless) Standard Model are listed in table 1, as ribbon diagrams on three strands, built with Dirac strings. Both massless neutrino helicities occur, but the other mirror braids are not listed. Observe the analogy between color and neutrino mass, as in the condensate CSFT scheme [22][23]. In the mirror set of diagrams we have the extra magnetic degrees of freedom, so that particles at the mirror carry dyonic charge.

The Chern-Simons action is applied to gravity in $2+1$ dimensions [44] using the Monster CFT of central charge 24. In motivic gravity, we build the mass gap for neutrinos, and there is a second CSFT for QCD and the strong CP problem [22][23]. The partition function of [44] is the modular j-invariant. Recall that this invariant is defined in terms of the Eisenstein forms E_4 and E_6, where E_4 counts roots on the $\mathbf{e_8}$ lattice. The j-invariant itself counts irreps for the Monster moonshine module, and its special real values include the golden ratio $\phi = (1+\sqrt{5})/2$ [45].

Compare the factor of 32 in (9) with the common normalisation of $1728 = 64 \times 27$. The $2048 = 64 \times 32$ equals $j(\pm\phi)$, and the set $\{\pm\phi, \pm\phi^{-1}\}$ is included in the critical set of real values of j. The conjugates of ϕ solve the quadratic in x which results from insisting on (i) the geometric sequence $F_{n+1} = xF_n$ and (ii) the Fibonacci recursion $F_{n+2} = F_{n+1} + F_n$. Thus ϕ is a placeholder for all rationals F_{n+1}/F_n.

To understand duality [7] we look at combinatorial degrees of freedom. Braids will be related to the associahedra. Two copies of $\mathbf{e_8}$ have 480 roots in

$$496 = 2(28 + 28) + 2(8 \times 8 + 8 \times 8 + 8 \times 8) \tag{10}$$

dimensions, giving 8 copies of 14 in the adjoint part. These are our *basis associahedra*. The octonion factors of 8 will be associated to 3-cubes, so that everything is encoded in dimension 4, since the tensor product corresponds to a sum of basis cube dimensions. More conventionally, the 14 trees label a 14 dimensional theory associated to the 3-time grading [46]

$$\mathbf{e_{8(-24)}} = 14 + 64 + (SO(11, 3) + 1) + 64 + 14. \tag{11}$$

Here the $64 = 35 + 21 + 7 + 1$ counts the ordered subsets of up to three distinct units in $e_1, \cdots, e_7$, and another 64 counts the subsets of size ≥ 4. That is, we have a 3-brane and magnetic 7-brane and the usual $SO(9, 1) \simeq SL_2(\mathbb{O})$ embeds in $SO(11, 3)$. As noted above, 7 dimensions means 7 ribbon strands, for a total of 14 braid strings. One may extend [46] this further to a $(19, 3)$ theory in the tower of exceptional periodicity. Eventually we find $SO(28, 4)$ breaking to $SO(3, 3) \times SO(25, 1)$, where 32 dimensions is high enough to obtain four copies of the integers $\mathbb{Z}^8/2$, used to define entries in $SL_2(\mathbb{C})$.

All higher dimensional associahedra are products of the polytopes in dimension 2 and 3 [47]. The three dimensional associahedron of figure 12 is a model for the sheaf cohomology of $\mathbb{RP}^2$. As is well known, the associahedra also describe the compactification of the genus zero moduli spaces $\mathcal{M}_{0,n}$ for Riemann spheres. At very high genus, which is relevant for H_2 homology in the smooth category, the moduli $\mathcal{M}_{\infty,1}$ has a completion $\mathcal{M}^+_{\infty,1}$ [48] such that

$$\pi_3(\mathcal{M}^+_{\infty,1}) = \mathbb{Z}_{24} + G, \tag{12}$$

for some G. Recall the stable group $\pi_{n+3}(S^n) = \mathbb{Z}_{24}$ for $n \geq 5$. Baez [48] describes $\mathbb{Z}$ as the decategorification of a category of tangles, where the objects are strings of n $\pm$ signs. Recall that 24 signs is the setting of the Golay code, underlying the Leech lattice [49][50]. Signs for tangles exist whenever duals are present, which is the case for all our categories.

Below we put braid group generators directly on the vertices of an associahedron. But there is another deep connection between links and the associahedra, as follows. Given any pair of rooted, binary trees t_1 and t_2 on d leaves, there is a pairing $h(t_1, t_2)$ which defines an element of Thompson's F group [51][52]. A traced pairing diagram built from t_1 and t_2 is a trivalent planar graph, whose edges may be colored with 3 colors such that each vertex carries one edge of each color. A $\pm$ sign is then attached to each vertex, as in figure 2, depending on whether the permutation of (123) is odd or even. The sign determines a link crossing when a trivalent vertex is extended to the crossing piece [52]. It turns out that *all links* may be obtained this way.

The four color theorem for planar maps is closely related to these questions, and the connection between this theorem and pentagons has a very long history. We show a 3-coloring of an associahedron in figure 11.

3.2. Qutrit rest mass eigenvalues

A *loop* is a quasigroup with an identity, in analogy to a category with a nonassociative product and noncommutative braiding. For example, the integral octonions form a finite nonassociative loop. Product tables for finite loops are Latin squares. Two simple examples of order 3 are the left unit loop and the idempotent loop,

$$L_{lu} = \begin{pmatrix} 1 & a & b \\ b & 1 & a \\ a & b & 1 \end{pmatrix}, \quad L_I = \begin{pmatrix} 1 & b & a \\ b & a & 1 \\ a & 1 & b \end{pmatrix}, \tag{13}$$

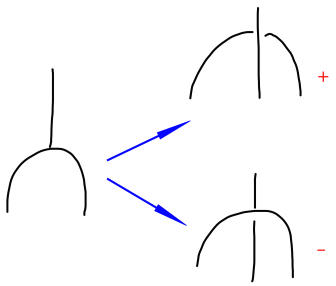

Figure 2. Trivalent vertex maps to link crossing

which are 1-circulant and 2-circulant symmetric, respectively. In general, an order 3 table is selected [53] from 9 points in the Hamming graph $H(3,3)$, which is the 27 points on the qutrit 3-cube (see below) of length 3 words on three letters $\{1,2,3\}$. For example, the pure state 221 puts a 1 in both the second row and second column of L_{lu}.

Hermitian 3×3 matrices in a generalised Jordan algebra are the natural place for rest mass triplets in the low energy regime. They are necessarily 1-circulants, belonging to a group algebra $\mathbb{F}S_3$ on the three object permutations, and diagonalised over $\mathbb{C}$ by the quantum Fourier transform (15). Similarly, a real 2×2 circulant has basis $\{1,\sigma_X\}$, where σ_X is the flip Pauli matrix of signature $(1,-1)$. We view either spacetime or momentum space [2] as a six dimensional entity, based on three 2×2 circulants, because under the action of the Lorentz group cover $SL_2(\mathbb{C})$

$$Q=\begin{pmatrix} n & m\\ p & q\end{pmatrix}\begin{pmatrix} a & b\\ b & a\end{pmatrix}\begin{pmatrix} q & -m\\ -p & q\end{pmatrix}=\begin{pmatrix} t+z & x+iy\\ x-iy & t-z\end{pmatrix} \tag{14}$$

is a vector (t,x,y,z) in Minkowski spacetime, with determinant $t^2-x^2-y^2-z^2$. Clearly it must be tripled to obtain the full (x,y,z) degrees of freedom.

When our ring R is eight dimensional over $\mathbb{Z}$, as above, three dimensional spaces are secretly 24 dimensional. We therefore expect fundamental phases like $\pi/4$ and $\pi/6$ [2]. These phases appear automatically in mutually unbiased bases [54][55][56] for qubits and qutrits. In a prime power dimension $d=p^r$ there are $d+1$ MUBs and $d-1$ mutually orthogonal Latin squares, like the pair above for $d=3$. More general Gauss sums for modular categories appear in [57], and the connection [58] to Frobenius algebras is discussed below.

Let $\omega=(-1+\sqrt{-3})/2$ be the cubed root of unity. The qutrit Fourier transform is given, up to permutations, by

$$F_3=\frac{1}{\sqrt{3}}\begin{pmatrix} 1 & 1 & 1\\ 1 & \omega & \overline{\omega}\\ 1 & \overline{\omega} & \omega\end{pmatrix}. \tag{15}$$

Its columns form one basis in a set of four MUBs for qutrits. The other 3 bases form a cyclic group $C_3\subset S_3$, and a cyclic group C_d appears in any prime power dimension $d=p^r$ [56]. The density matrices of these columns are the idempotents

$$B=\frac{1}{3}\begin{pmatrix} 1 & \omega & \overline{\omega}\\ \overline{\omega} & 1 & \omega\\ \omega & \overline{\omega} & 1\end{pmatrix},\ C=\frac{1}{3}\begin{pmatrix} 1 & \overline{\omega} & \omega\\ \omega & 1 & \overline{\omega}\\ \overline{\omega} & \omega & 1\end{pmatrix},\ A=\frac{1}{3}\begin{pmatrix} 1 & 1 & 1\\ 1 & 1 & 1\\ 1 & 1 & 1\end{pmatrix}, \tag{16}$$

and a Hermitian mass operator is a combination of these idempotents. Let

$$\sqrt{M}=aA+bB+cC \tag{17}$$

for a, b, c real. Our masses are the squares of the three eigenvalues of $\sqrt{M}$, accounting for the chiral components of our mass states. Without loss of generality, fix a mass scale by the rule $(a+b+c)^2 = 1$. The Koide rule [59][60] follows from the eigenvalues of the charged lepton matrix

$$\sqrt{M} = \frac{\sqrt{\mu}}{\sqrt{2}} \begin{pmatrix} \sqrt{2} & \theta & \overline{\theta} \\ \overline{\theta} & \sqrt{2} & \theta \\ \theta & \overline{\theta} & \sqrt{2} \end{pmatrix}, \tag{18}$$

where the scale $\mu = 4/3$ follows from $(a+b+c) = 1$. For charged leptons, the 4 in μ rescales to the mass of the proton, and the observed value of θ is close to $2/9$. The quarks have mass matrices whose phases are $1/3$ and $2/3$ of this value. The observed neutrino scale is around 0.01 eV, and its phases are $2/9 \pm \pi/12$ [2][61].

We embed our Hermitian elements from $J_3(\mathbb{C})$ in a higher dimensional exceptional Jordan algebra [2]. Recall that triality acts on the three off-diagonal copies of $\mathbb{O}$ in a 3×3 element of $J_3(\mathbb{O})$, and all circulants belong to a group algebra for the permutations S_3, which is our basic Hopf algebra [62]. Mass matrices use the cyclic group $C_3 \subset S_3$, and diagonal mass triplets are functions on C_3, so that under the Fourier transform the quantum double $D(S_3)$ of S_3 looks like an algebra $\mathbb{F}C_3 \otimes \mathbb{F}C_3$, in which electric magnetic duality will become completely transparent.

The Fibonacci B_3 representation is 2×2, fitting in three ways into a generic 3×3 unitary matrix. A circulant mixing factor is automatically in $SU(2) \times U(1)$, and the product of F_3 and the real form of the tribimaximal matrix gives a 3×3 representation [61] of the arithmetic phase $\pi/12$. Under Fourier supersymmetry [1], neutrinos are mapped to the photon identity braid, while $e^{\pm} \mapsto W^{\pm}$. The Z boson is associated to the choice of twist for the Fourier transform. There is no need for any particles beyond the SM, and the $\pm\pi/12$ phase is analogous to the phase for the weight $1/2$ Dedekind η function. Fibonacci categories have doubles, which are a natural setting for our mirror pairs.

Table 1. Standard Model electric braid states

	L	R	$(1)_{L/R}$	$(2)_{L/R}$	$(3)_{L/R}$
ν	$\sigma_1\sigma_2^{-1}$	$\sigma_2^{-1}\sigma_1$	m_1/N_1	m_2/N_2	m_3/N_3
$\overline{\nu}$	$\sigma_1^{-1}\sigma_2$	$\sigma_2\sigma_1^{-1}$	N_1/m_1	N_2/m_2	N_3/m_3
e^-	$(---)$	$(---)$			
e^+	$(+++)$	$(+++)$			
$\overline{u}$			$(--0)$	$(0--)$	$(-0-)$
d			(-00)	$(0-0)$	$(0--)$
u			$(++0)$	$(0++)$	$(+0+)$
$\overline{d}$			$(+00)$	$(0+0)$	$(00+)$

To give the local charged leptons mass through emergent Yukawa couplings, we need a (GUT) quark neutrino complementarity, swapping color and chirality, explaining why chirality is represented in B_3. The Fourier transform is associated to geometric duality in our 4-categories, where a braided monoidal representation category has 2-arrows, 3-arrows and four dimensional axioms.

Under chiral symmetry breaking, fermion pairs create the Bose-Einstein condensates of the quantum vacuum. Our central right handed neutrino mass corresponds to the present day CMB temperature at 0.00117 eV, indicating that the CMB is direct evidence for a condensate cosmology.

4. The categorical perspective

4.1. Beyond set theory

Axiomatically, quantum gravity is about categorical logic for propositions about the quantum vacuum, whose structure begins with the cosmological neutrino ansatz [1][2]. Recall that classical logic employs sets and distributive lattices, where Stone's theorem [63] states that the space associated to a lattice is Hausdorff if and only if the lattice is Boolean, defining a category of Stone spaces, which is a special limit of the category of finite sets. Ordered Stone spaces are essentially *coherent* spaces, and coherent locales are essentially locales of ideals in a distributive lattice. Distributive lattices are Boolean only if all prime ideals are maximal. In short, classical spaces are derived from lattice algebras with a number theoretic flavour.

Quantum mechanics immediately requires nondistributive lattices, and axioms for higher dimensional categories [64][65]. The polytopes of scattering theory [65] associate particle number with dimension, naturally introducing infinite dimensional categories, starting with the 1-operad of the associahedra. The category of Hilbert spaces for quantum mechanics is a symmetric monoidal category, but for gravity we permit a non trivial braiding.

Replacing the Boolean truth values $\{0, 1\}$ with $\mathbb{R}$ takes us from Stone duality to either Gelfand duality (for commutative rings) or $\mathbb{R}/\mathbb{Z} = S^1$ in Pontryagin duality. But we need not give S^1 a real structure immediately when algebraic number fields are in play, so long as we note that S^1 should contain a copy of every cyclic group. Quantum mechanical propositions localise to definite rational prime powers, like $p = 2^2$ for two qubits. Only a maximal category of all possible state spaces would require a notion of real number. Thus our braid loops are not at all S^1 spaces in the usual sense.

For nonperturbative structures, we need a monadic connection between algebra and geometry, defining endofunctors on true categories of motives. If a ring R is commutative, its set of idempotents forms a Boolean algebra, and any commutative R is a ring of global sections for a sheaf on a Stone space [63]. The canonical such sheaf is the *Pierce sheaf*, based on the Stone space spec $I(R)$, where $I(R)$ are the idempotents of R. Pierce decompositions extend to noncommutative and nonassociative algebras based on $\mathbb{H}$ and $\mathbb{O}$. In particular, the integral part of the exceptional Jordan algebra $J_3(\mathbb{O})$ plays a key role in motivic gravity [2][46][66].

Nondistributive lattices in ordinary quantum mechanics are usually commutative, because for vector spaces the unions $V \wedge W$ are commutative. Tensor products are also weakly commutative in the symmetric monoidal structure, just as Cartesian products are for sets. Our braidings break this symmetry, and this characterises the particle spectrum of the Standard Model. Distributivity is discussed further in the last section.

4.2. Frobenius and Hopf algebras

Mutually unbiased bases [54][55][56] and related observables in ordinary quantum mechanics are associated to algebra objects in a symmetric monoidal category. A pair of complementary observables [58] determines a pair of interlaced Frobenius algebras, which form Hopf algebras as follows.

A dagger symmetric monoidal category has an involutive functor $\mathcal{C}^o \to \mathcal{C}$ which equals the identity for objects, and an arrow f is self-adjoint if $f^\dagger = f$. In a strict monoidal category $\mathcal{C}$, we consider the subcategory $\mathcal{P}$ generated under $\otimes$ by a single object. For example, take all qubit spaces in the category of finite dimensional Hilbert spaces. Since the objects in such a subcategory are labelled by $\mathbb{N}$, it is called a PRO. A strict monoidal functor $\mathcal{P} \to \mathcal{C}$ will be called a $\mathcal{P}$-algebra (the usual term is T-algebra, but this has multiple meanings for us). If there is a symmetric group action, a PRO is known as a PROP.

Now consider a PROP for commutative monoids, generated by an object P. There are multiplications $\mu : P \otimes P \to P$ and unit maps $\eta : 1 \to P$, where as usual μ is depicted as a trivalent vertex and associativity holds. Anything can be weakened in higher dimensions, but

this is a reasonable setting for quantum mechanics. The cocommutative comonoids have upside down diagrams, with a coproduct $\delta : P \to P \otimes P$ and counit $\epsilon : P \to 1$.

We care about the PROP [58] for *commutative Frobenius algebras*. These are bialgebras $(\mu, \eta, \delta, \epsilon)$ such that string duality holds on the 4-valent diagrams $\delta\mu : P \otimes P \to P \otimes P$. If it is also the case that $\mu\delta = 1$, the algebra is *special*. For the special commutative Fronenius algebras in a dagger category, the *spider theorem* [67] says that all tree components (both upward and downward pointing arrows $P^n \to P^m$) collapse to a single vertex, so that the fusion trees are unimportant. This PROP is equivalent to the category of cospans on finite sets.

It turns out that we have a *dagger special commutative Frobenius algebra* exactly when an orthonormal basis $\{p_i\}$ for P satisfies

$$\delta_1 : p_i \mapsto p_i \otimes p_i, \quad \epsilon_1 : p_i \to 1 \tag{19}$$

for all i. That is, a basis vector is grouplike for the coproduct, meaning that it is copied like a classical operation. Our quantum monad for gravity is motivated by this concrete description of measurement, which singles out set like objects in a basis. For a Hilbert space of dimension n, let $i, j \in 0, 1, \cdots, n-1$. Then there is an algebra with $\mu_2 : p_i \otimes p_j \mapsto p_i + p_j$ and $\eta_2 : p_0 \to 1$. It is only weakly special, as $\mu\delta = n \cdot 1$, bringing in the normalisation factors for MUBs.

Another important coproduct, written here for a finite abelian group, is $\delta_2 : g \mapsto \sum_{a+b=g} a \otimes b$. The pair (μ_2, δ_2) form a Frobenius algebra. For quantum complementarity, the trick is to mix up the algebras and coalgebras on a Frobenius diagram, because with a Fourier transform, we are interested in interacting observables. So we color the μ vertex differently from the δ vertex, and the two mixed algebras (μ_1, δ_2) and (μ_2, δ_1) are Hopf algebras. For example, for a finite abelian group, (μ_2, δ_1) is the group algebra and (μ_1, δ_2) applies to group characters. Coproducts of the form δ_2 underlie the construction of Jordan algebra pairs. In these commutative Hopf algebras, the antipode always satisfies $S^2 = 1$.

For condensation in gapped boundary systems, where fusion becomes important, we permit a weakening of such structures, but the algebra object remains commutative, as we would expect for an observable that manifests itself in classical reality.

4.3. The pentagon of trees

Let us return to the basics of polytopes and braids. A finite dimensional module over a ring R typically has a basis set. For example, figure 1 is the lattice of subsets for a three element set $\{I, J, K\}$, which form a basis for space. Here we have reduced the 8 dimensions of $\mathbb{O}$ to a 3 dimensional object, whose seven non trivial units give the Fano plane. Given a three element set $\{I, J, K\}$, its subsets are generated by the polynomial

$$(x + I)(x + J)(x + K), \tag{20}$$

and similarly for any n point set. Setting $I = J = K = 1$ recovers the binomial coefficents, which generalise to the Gaussian polynomials when $I = 1$, $J = t^2$, $K = t^{-2}$. For four variables, the Gaussian polynomials come from $\{t^{-3}, t^{-1}, t, t^3\}$, and so on. Thus polynomials in more variables may be obtained when I, J and K are not fixed in the usual fashion.

For quantum logic, elements are initially lines, rather than points. In figure 3, we replace words by line configurations. Each letter represents an intersection point, so if we look at the intersection points on the lines, the double letters (IJ etc.) disappear from the cube, leaving a 5-cell of five points. Such 5-cells often appear in higher dimensional lattices.

A planar projection of a 5-cell is a pentagon. The pentagon of figure 4 carries a variety of labellings. As the first polytope in the sequence of associahedra, it's vertices are the binary rooted trees with five leaves, including the root. The noncommutative forests are easily derived from

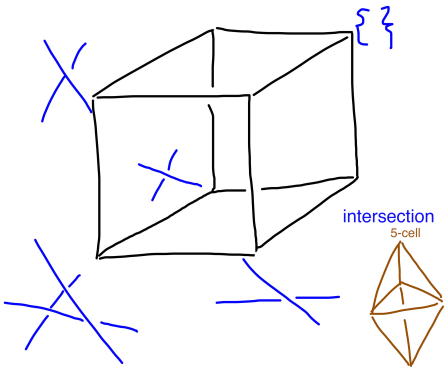

Figure 3. 5-cell from three lines

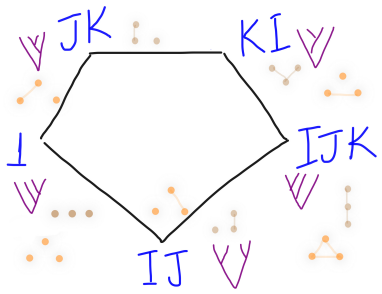

Figure 4. The pentagon vertices as (i) binary rooted trees (purple) (ii) noncommutative forests (brown) (iii) non-crossing partitions (orange)

the trees by looking at the areas between the tree edges. These labels exist for the associahedron in any dimension.

Another natural labelling of the pentagon uses elements of the braid group B_3, which has generators σ_I and σ_J satisfying the group law

$$\sigma_I \sigma_J \sigma_I = \sigma_J \sigma_I \sigma_J. \tag{21}$$

Observe how the blue words on the pentagon match the non-crossing partitions of the dot triangle, when the vertices on the triangle are labelled I, J, K. Now we use the letters I, J and K to represent elements of B_3 and include other elements of B_3 to cover all vertices of the pentagon. A non-crossing partition indexes a braid [68][69] when the partition is assigned a permutation in S_3, such that the identity 1 is the source of the pentagon, as shown. Given 3 points in a disc, the permutation looks at the triangle defined by the 3 points and says where the braid will send each point around the triangle.

In this way, the braid group B_n in any dimension is mapped to the vertices of the associahedron in dimension $n-1$, and the generators of B_n are mapped to initial directions on the polytope. Our ribbon charges correspond to vertices on the cubes, and we combine all relevant polytopes in a higher dimensional operad for ribbon diagrams.

4.4. Fibonacci braids and condensation

An example of a cyclic B_3 representation in $\mathbb{H}$ is [70]

$$\sigma_{12} = \frac{1}{\sqrt{2}}(1+i), \quad \sigma_{23} = \frac{1}{\sqrt{2}}(1+j), \quad \sigma_{13} = \frac{1}{\sqrt{2}}(1+k). \tag{22}$$

The pentagon also includes the identity 1 and the product $\sigma_{12}\sigma_{23}\sigma_{13}$. Under the Pauli matrix representation for $\mathbb{H}$ we have

$$\sigma_{12}\sigma_{23}\sigma_{13} = \frac{\mathbf{i}}{\sqrt{2}}\begin{pmatrix}1 & 1\\ 1 & -1\end{pmatrix}, \tag{23}$$

which is the Fourier transform. A rotation of this representation in $SU(2)$ takes us to the Fibonacci anyon representation, which is 2×2 for B_3. Consider now the closely related 3×3 cyclotomic representation of the four strand braid group B_4 in [71], namely

$$\sigma_1 = \begin{pmatrix} e^{3\pi i/5}+\phi e^{-3\pi/5} & 0 & 0\\ 0 & e^{3\pi i/5} & 0\\ 0 & 0 & e^{3\pi i/5}\end{pmatrix}, \tag{24}$$

$$\sigma_2 = \begin{pmatrix} e^{3\pi i/5}+\phi^{-1}e^{-3\pi i/5} & 0 & \phi^{-1/2}e^{-3\pi i/5}\\ 0 & e^{3\pi i/5} & 0\\ \phi^{-1/2}e^{-3\pi i/5} & 0 & e^{3\pi i/5}+e^{-3\pi i/5}\end{pmatrix},$$

$$\sigma_3 = \begin{pmatrix} e^{3\pi i/5} & 0 & 0\\ 0 & e^{3\pi i/5}+\phi^{-1}e^{-3\pi i/5} & \phi^{-1/2}e^{-3\pi i/5}\\ 0 & \phi^{-1/2}e^{-3\pi i/5} & e^{3\pi i/5}+e^{-3\pi i/5}\end{pmatrix}.$$

A similar representation exists for all B_n with $n\geq 3$ in a dimension given by the corresponding Fibonacci number, and is universal for quantum computation. The qutrit components for the Fibonacci anyon are labeled by the words IX, XI and II, where I and X are the two objects and $X\otimes X\simeq I+X$ is the non trivial fusion rule.

Thinking of dissipation for thermal gravity, note that Fibonacci fusion is an example of near-group fusion [72] on a not necessarily invertible object X, namely

$$X\otimes X\simeq G+kX, \tag{25}$$

for a group G and ordinal k. For $|G|=k+1$, the category exists only when G is the multiplicative part of a finite field, the cyclic group C_{p^r-1}. Examples of interest include $(G,k)=(C_2,1)$, which has three $\otimes$ structures [72], and $(C_{p-1},p-1)$ for a prime p, which defines a sequence Fib_p of Fibonacci categories, starting at $p=2$. At $p=3$ we obtain the rule

$$X\otimes X\simeq I_1+I_2+2X, \tag{26}$$

where we write I_1 and I_2 for the objects in G. This is known as the $\mathbf{e_6}/2$ rule. The prime p corresponds to the qudit points on a discrete cube, where the usual parity cubes give qubit states on 0 and 1. Targets of parity cubes also represent square free ordinals. The trit at $p=3$ gives a divided cube whose dimension is fixed by the number of X letters in a word. For example, the 9 point square holds all words with only one X, such as I_1XI_1 at 11 or I_2X at 20.

Hopf algebras graded by G generalise supersymmetry [73], which we see here at $p=3$. Here the object $I_1+(I_1+I_2)$ in the category of vector spaces has a unique C_2-graded Hopf structure which is a quotient of $\mathbb{C}[x,y]$ with an antipode $S(x)=x$ and $S(y)=-y$. The category of C_2 graded vector spaces is thought of as a condensation of the modules for the Hopf structure, which happen to give the category of representations of the permutation group S_3. Recall that the double $D(S_3)$ governs electric magnetic duality, as discussed below.

The ordinary Fibonacci category Fib_2 is a condensation of its double category, with special object $2I+X$ [73]. In this case we have an unconventional antipode satisfying $S^{10}=1$, where

$$S=\mathbf{1}_{I_1}+\mathbf{1}_{I_2}-\frac{\phi^{-1}+\rho i}{2}\mathbf{1}_X, \tag{27}$$

with $\rho = \sqrt{\phi + 2}$.

By definition [73], an algebra object A in a braided fusion category is *condensable* if (i) $m\sigma_{UV} = m$ is commutative (ii) $\mathrm{Hom}(1, A)$ is equivalent to the underlying field, and (iii) the multiplication m comes with a splitting map $A \to A \otimes A$. Compare this to the commutative Frobenius algebras. The only new thing is connectedness, condition (ii), which is true for Hilbert spaces by linearity. A condensation functor $\mathcal{C} \to \mathcal{C}_A$ has a right adjoint, and the composition of adjoints is a Hopf comonad. Thus condensation is the correct setting for the quantisation of classical monads, such as the power set monad for classical logic.

A monad T with its structure map $T^2 \to T$ is the ultimate generalisation of an idempotent for measurement. Abstract condensation is encoding the collapse of the wave function. Observe how the Fibonacci fusion rule $X \otimes X \simeq X \oplus I$ may be interpreted: as a projective idempotent of the form $X^2 = IX$.

Now consider ribbon representations, starting with representations for the quantum double of a finite group. These categories arise with the condensation of anyons to a surface boundary. A hexagonal lattice is considered in [7], but the arguments apply to any lattice. The Dijkgraaf-Witten model in [9] uses an inner and outer rectangle of plaquettes in a square lattice for a discrete $G = S_3$ gauge theory, with an initial Kitaev Hamiltonian. Here a ribbon is a chain of simplices in the lattice, and each simplex carries a qudit. The ribbon operators on the lattice form a Hopf algebra dual to $D(G)$.

Gapped boundary types correspond to subgroups of G, such as our $C_3 \subset S_3$. Recall that $D(C_3)$ uses the Fourier transform F_3 to make electric magnetic duality manifest [62]. As explained in [7], the trivial subgroup gives electric charge condensation, while the fullgroup G gives flux condensation. Elementary excitations in general, here for a finite group G [9], are dyonic pairs (m, e), where the magnetic charge m is a conjugacy class for G and the electric charge e is an irrep for its centraliser. In other words, a dyon is an irrep for the quantum double. For example, $m = \{(231), (312)\}$ and $e = C_3$. This explains the choice of particle braids in table 1.

Anyon fusion occurs when two excitations are brought to the same simplex on the lattice. Compare this to figure 7, where two types of overlap triangle are possible. In defects on the boundary, these two options define two distinct tensor products. A gapped boundary in [9] is a condensable algebra object $\mathcal{A}$, in a unitary modular tensor category, which is also Lagrangian, meaning that the quantum dimension of $\mathcal{A}$ is the square root of the full category dimension.

A collection of n gapped boundaries (internal rectangles on the lattice) models n marked points on a Riemann sphere, and hence n anyons for the fusion trees on the associahedron with n leaves. A sequence of splittings from the vacuum object, followed by condensation of n objects to the vacuum, is exactly a choice of two trees on the associahedron, which defines an element of Thompson's F group, as described in section 3.1. These are ground state degeneracies. Thus two boundaries $\mathcal{A}_1$ and $\mathcal{A}_2$, along with the vacuum, define a pair of pants diagram, and in this case a bulk anyon particle/antiparticle pair (which condenses) may be represented by a (Wilson) line connecting the two holes on a surface.

Condensation introduces $3j$ symbols into the structure [7] of the category, generalising triality on $V_1 \otimes V_2 \otimes V_3$. Its equation compares two diagrams: one that first fuses two bulk anyons and then condenses them onto a boundary, and one that condenses two anyons separately. The symbols have six indices: three for the $2+1$ bulk anyons and three for the condensation vertices on both diagrams, where the latter are basis indices for the V_i. The required axiom is a pentagon with four $3j$ arrows and one fusion arrow [9], and the commutativity of condensation relates the $3j$ to the braiding operator. Finally, a $6j$ symbol is defined across the boundary by a mirror pair of $3j$ equations, summing over both the input bulk fusion and the mirror fusion index. In [7], a trivalent vertex is built using a $3j$ symbol, but our boundaries [9] make 4-valent graphs, which turn into associator trees on the selection of a root leaf. Thus the pentagon is essentially

Mac Lane.

Our 3×3 algebras for B_4 are augmented by MUBs for Dirac operators, including a 4×4 Fourier MUB for the γ_5 matrix. This now appears in the Lie algebraic triality automorphism τ for D_4 in terms of the modular S and T matrices for the toric code fusion category, for which $G = S_2$ in the above. That is,

$$-2\tau = ((41)(32)) \circ S \circ T = \begin{pmatrix} 0 & 0 & 0 & 1 \\ 0 & 0 & 1 & 0 \\ 0 & 1 & 0 & 0 \\ 1 & 0 & 0 & 0 \end{pmatrix} \begin{pmatrix} 1 & 1 & 1 & 1 \\ 1 & 1 & -1 & -1 \\ 1 & -1 & 1 & -1 \\ 1 & -1 & -1 & 1 \end{pmatrix} \begin{pmatrix} 1 & 0 & 0 & 0 \\ 0 & 1 & 0 & 0 \\ 0 & 0 & 1 & 0 \\ 0 & 0 & 0 & -1 \end{pmatrix}. \tag{28}$$

The 4-basis is $\{1, e, m, em\}$ [9], and the Lagrangian algebras are $\mathcal{A}_1 = 1 + e$ and $\mathcal{A}_2 = 1 + m$. Flux condensation sends 1 and e to 1, and m and em to m, and the braiding moves one hole around another.

The usual Fibonacci category is a condensation of its double. The representation of B_n in (24) comes with a ribbon twist map $\theta_X = -e^{\pm \pi i/5} 1_X$. We assume that the $\sqrt{\phi}$ appears as a Lagrangian dimension for some higher dimensional structure, and the antipode of (27) also requires rings with the number ρ, as expected. Recall that the scale factors $(1, \phi)$ are associated to one copy of $\mathbf{e_8}$, introducing a $(4, 4)$ metric under the negative norms involving ϕ.

Consider twisted doubles. For the cyclic group C_2 of the toric code, it is shown in [74] that one 3-cocycle $C_2 \times C_2 \times C_2 \to U(1)$ takes the value -1 on the target (111) of the parity cube, and the value 1 elsewhere. The ground state degeneracy is 4, and these signs determine the 2×2 Fourier transform. This defines a twisted double lattice model, whose string dual is the Levin-Wen model for the quantum group $U_q(sl_2(\mathbb{C}))$ when $q = \omega$. Recall that $q = \omega$ has two simple reps, while the category at the fifth root of unity has four. For C_3, there is only one twisted double with a Levin-Wen dual, whose cocycle defines the nine entries of the Fourier matrix F_3. But there are two other cocycles [74] for C_3 with a ground state degeneracy of 9, including one based on the topological phase $\theta = e^{2\pi i/9}$.

Recall the planar pants diagram, with a bulk anyon line connecting the two interior circles. A pair of S^1 circles is a toric analog of the pair of S^2 which form a 1-handle in a Kirby diagram. Thus a single bulk anyon ribbon is a natural surface analog of the cancelling 2-handle, and for both T^2 and $S^2 \times S^2$ the 2×2 intersection form is given by σ_X in (6). The torus is the compactification of the $(1, 1)$ Minkowski plane, while $S^3 \times S^3 \subset \mathbb{R}^8$ compactifies our $(3, 3)$ space.

Thus we interpret the three copies of σ_X in (7) as three gapped boundaries for mass generation. Then for $D(C_3)$ we have two condensates: $1 + e + \overline{e}$ and $1 + m + \overline{m}$. This category is the same as $SU(3)_1 \times \overline{SU(3)}_1$, which we can represent with two surface layers, so that the bulk line between two holes is categorified to a cylinder handle connecting the holes on different sheets. Sliding tubes past each other in this 3-space is like wormhole braiding, and the dimension of the theory has been raised. For one cylinder, say connecting an e^+e^- pair, we consider a ribbon strip in a CFT as a boundary of the bulk cylinder.

Given a two dimensional cylinder of radius r, which is $\mathbb{CP}^1/\{0, 1\}$, we define a CFT energy momentum tensor for a periodic strip of width $2\pi r$ in the plane [75]. The anomalous

$$\langle T \rangle = \frac{c}{24r^2} \tag{29}$$

is due to the finite size, as in a Casimir effect for the two edges, thought of as horizons in opposite directions. When the two horizons are free, this is reduced by a factor of 4. In dimension four, quantum inertia [76][77] is a Casimir effect for two celestial horizons [2]: the local Rindler horizon and the cosmological horizon of the EW vacuum. For very low accelerations the rest mass is reduced, and it becomes zero at an Unruh wavelength of $4R$ for $R = \pi r$ the Hubble radius.

The factors of π that often appear (in comparing circle clocks to radial clocks) are hypothesised to be responsible for an exact Koide 2/9 parameter. For instance, in $2/9 = (2\pi/27)(3/\pi)$ the second factor is an exact effective dark mass-energy fraction, derived from the Friedmann equation using a semiclassical pair production argument [78]. Since we are working beneath classical equations, the 2/9 might arise fundamentally as $(2\pi/9)(1/\pi)$, with the $2\pi/9$ appearing above as the cocycle for the C_3 twisted double [74]. This deserves further investigation, especially since the critical strip of the Riemann zeta function $\zeta(s)$ has an inertial line at $s = 1/2$.

4.5. Templates and ribbons

Categorification is inevitable in quantum computation, where lines are thickened to ribbon strips, used to build surfaces with boundaries. A *template* is a branched surface which includes ribbon vertices, as shown in figures 5 and 6. In 1995, Ghrist [79] showed that there exists a template with four holes containing *all* knots and links, as one would expect for a DNA code.

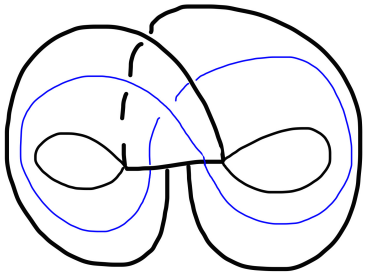

Figure 5. A two-holed Lorenz attractor with blue path

Everything happens in either three or six dimensions, because the higher dimensions of extended M theory just correspond to extra strands in our braid diagrams. This has been discussed elsewhere. Figure 6 illustrates the standard product and coproduct diagrams for a bialgebra, reading the processes down the page. Templates [80] also include up and down ribbon caps for duality, as in the Lorenz template of figure 5.

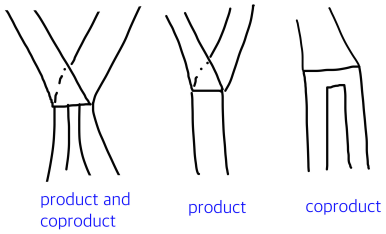

Figure 6. Template vertices

A template diagram has a framed link equivalent, as shown in figure 7. Kirby moves act on the framed links.

For the B_3 diagrams, there exists a universal representation of $SU(2)$ using the Fibonacci anyons [71][81]. Our Standard Model particle braids [82][65][38][39] assign $SU(3)$ color to a choice of one in three twisted ribbon strands, and the twist is a $U(1)$ charge, as in table 1.

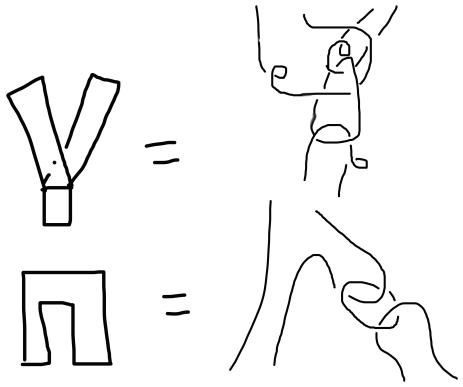

Figure 7. Framed links for template vertices

4.6. Simplices and polytopes
A discrete cube is a finite piece of the integral lattice with d points along each edge segment. Its vertex coordinates are noncommutative words in the integer letters. For commutative coordinates, we take diagonal slices. For example, the two words (10) and (01) sit at either end of a diagonal line across the square in the plane. We replace letters with the variables X and Y, so that the integers count the number of appearances of X and Y in a word. Then X and Y are directions in space. For a three letter qutrit alphabet, we get 2-simplices, as in the examples of figure 8.

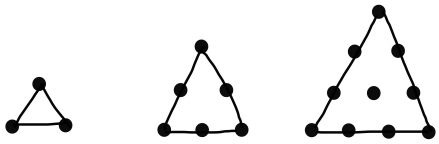

Figure 8. Discrete simplices on three letters

A pentagon has natural integer coordinates [83], as in figure 9, so that three pentagons sit inside the tetractys simplex on the right. Observe the correspondence between these coordinates and words on the pentagon of figure 4. We can do this for the associahedron in every dimension, using discrete simplices with $d + 1$ points on each edge.

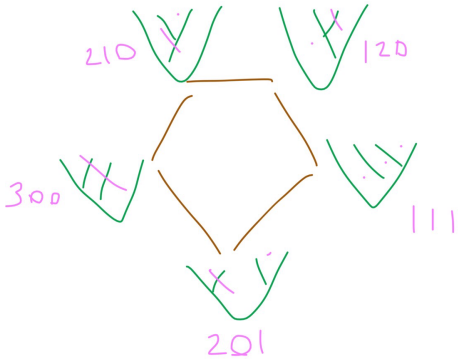

Figure 9. Coordinates for a pentagon

The associahedron of figure 11 has 14 vertices, and 24 triangular faces when each of its six pentagons is divided into three triangles. When all faces are triangulated, the associahedron is dual to the 24 vertex permutohedron for S_4. Coordinates for the associahedron are extended [1] to the 120 vertex polytope of figure 10, which is a pentagon blow up of the permutohedron. Two copies of this polytope catalog the 240 roots of $\mathbf{e_8}$ in dimension 4, where the scaling factors $(1, \phi)$ come from the icosian integers. The $\mathbf{e_8}$ roots in the magic plane attach Jordan algebra elements to the six points of the star [66], lying inside the six points of its $\mathbf{a_2}$ plane. These are the 12 points of $\mathbf{g_2}$ coming from the vertices of the cuboctahedron on the three qutrit cube.

Again, the 24 vertices of the permutohedron are each blown up in the 120 vertex permutoassociahedron of figure 10. Let us divide the 24 pentagons into two sets, green and red. The green lines connecting the 12 green pentagons form the icosahedron, with 20 triangular faces.

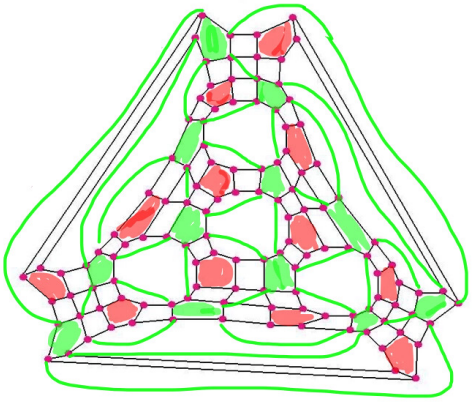

Figure 10. Icosahedron inside the permutoassociahedron

The 12 vertices of the icosahedron have traditional coordinates of the form $(0, \pm 1, \pm\phi)$, with cyclic permutations. The 6 lines through a centred pentagon on the icosahedron come from a 6 dimensional lattice. In figure 10, the 8 green triangles inside a 12-gon form a square on 8 out of 20 vertices of the dodecahedron. These are the vertices $(\pm 1, \pm 1, \pm 1)$, where the other 12 coordinates are cycles of $(0, \pm\phi, \pm(\phi - 1))$. The 12 vertices of the icosahedron are similar to the 12 vertices of the cuboctahedron, inscribed on the 12 edges of a cube.

The golden number ρ appears in the right angled triangle with an angle of 36° and side lengths $(\sqrt{5}, 2\rho, \phi\rho)$. A pentagram component is the right angled triangle $(1, \sqrt{\phi}, \phi)$. To include $1/\sqrt{\phi}$, as in (24), we need integers of degree 8, or 16 with the complexification of (27).

A discrete direction in our computational space is labelled by the toric paths 1, X, XX, and so on. Given the qudit interpretation, we want an auxilliary space whose directions are given by prime powers, so that all qubit cubes are given by a discrete edge, as in the sides of triangles in figure 8. The figure 8 simplices then belong to higher dimensional qutrit cubes, where the dimension is determined by the number of letters in the word labelling a point. Thus as usual the commutative tetractys diagram gives the 27 points on the 3-cube. The central word XYZ holds 6 permutations for the six paths on the little cube with target point XYZ. But in dimension 4, the 81 path 2-simplex now labels points on a 4-cube. So we can either increase the number of points along an edge in dimension p, and take the diagonal simplex, or we can fix p points on an edge and increase the dimension. In the former case, the dimension is constrained by the qudits, and four dimensions carries 4-simplices for 5-dits, while two dimensions carries the qutrits.

Introducing the prime 7 in dimension six, we get the cubicuboctahedron and the Mathieu

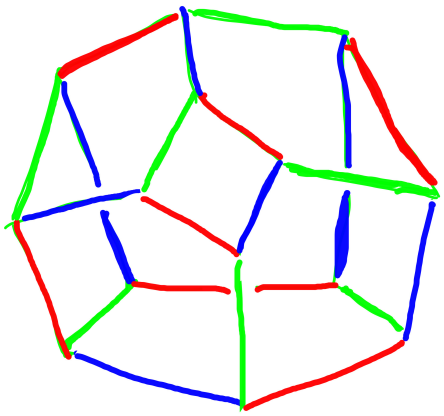

Figure 11. 3-coloring of the associahedron

group M_{24} [84], starting with a permutoassociahedron model for the genus 3 surface. The seven primes (including 1) p that divide the order of M_{24} are precisely those such that $p+1$ is a divisor of 24. M_{24} has 26 irreps, and their dimensions satisfy nice properties. Only the largest irrep, at dimension 10395, has a new prime factor, namely the 24th prime 83.

5. Motivic pairings

PROP categories rely on a higher dimensional notion of distributivity [58][85]. For quantum logic, where set cardinality is replaced by dimension, the reals are automatically infinite dimensional, and we would like to think of distributivity in ∞-categories. Here however, it depends on a braiding between $\otimes$ and $\oplus$ structures.

Observe that while all $n \in \mathbb{N}$ have a unique prime factorisation, all $n \in \mathbb{N}$ also have a unique sum decomposition $\sum_i F_i$ into non consecutive Fibonacci numbers. So we think of the ∞-category distributivity in terms of maps between the product and sum representations. Morally, this canonical category of motives underlies L-functions, like the Riemann zeta function. The B_i matrix representations under $\oplus$ have increasing dimensions F_i inside B_n, while there is a state space of dimension $n = p_1^{r_1} \cdots p_k^{r_k}$ under $\otimes$.

Quantum distributivity fills in higher dimensional cells. The union of lines I and J is the plane IJ, suggesting a square face on a cube, or pseudonatural transformation. In our double 4-category, 2-arrows are objects in two different ways.

All computations are motivic. An integral is generically a pairing between universal homology and cohomology. The isomorphism between these spaces is natural when objects have both a geometric and algebraic interpretation, wherein our topological field theories become monadic endofunctors. Such a pairing is generically a functor $F : \mathcal{C}^o \times \mathcal{C} \to \mathcal{R}$, so that a map between two such functors F and G is a dinatural transformation α [86], which satisfies the hexagonal rule

$$F(D,C) \to F(C,C) \to^{\alpha_C} G(C,C) \to G(C,D) = \tag{30}$$
$$F(D,C) \to F(D,D) \to_{\alpha_D} G(D,D) \to G(C,D)$$

for every $f : C \to D$ in $\mathcal{C}$. So it's basically a natural transformation for the spans and cospans on an original category of sets. Given such a functor F, a *coend* of F is a pair (C, α), with C an object and α a dinatural transformation $F \to C$ that maps F to a constant.

Let C be a coend in a ribbon category $\mathcal{C}$. A *Kirby element* in a ribbon category [87] is a morphism $f : 1 \to C$ such that any framed link L on n strands defines a good invariant $T(L, f) = a_L \circ f^{\otimes n}$, where $a_L : C^{\otimes n} \to 1$ is the unique arrow that attaches the link to an object

$X_1 \otimes \cdots \otimes X_n$. In a ribbon fusion category, with a finite set s of simple objects, a coend has the form $C = \oplus_{i \in s} X_i^* \otimes X_i$. In the double Fibonacci category Fib_2, this gives us the special object $2I + X$.

Under the Thompson group construction of section 3.1, a fusion vertex can become a braid crossing on a link. But we can never obtain a 3-coloring at a vertex in the Fibonacci category. In a category where we can have three colors at a vertex, like an annihilation $(e, \overline{e}, 1)$ interaction vertex, the bulk fusions in a ground state $1 \to 1$ diagram are removed, and there are no vertices in the resulting link diagram. If the initial crossings lie inside a set of holes on the link diagram, the hole boundaries are then connected by non crossing lines, as for planar algebra diagrams. We see then that these holes add structure to the local cutouts used in skein relations.

Finally, figure 12 is a heuristic view of a proper helicity neutrino at the Thompson scattering mirror, with a collapsed RH braid representing the sterile state of the CMB.

The moral of the story is that motivic geometry cares about numbers. We do not start with messy real or complex analysis, or classical gauge groups, since these methods rightly exist only as a limit of local (meaning at a prime) computational diagrams.

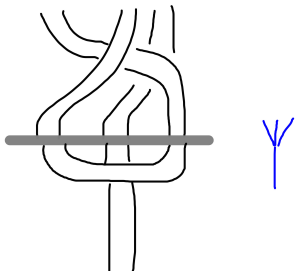

Figure 12. Neutrino braid at mirror with RH line

Acknowledgments
The author thanks Vaughan Jones for speaking about the Thompson group trees in Auckland, some time in 2016.

Appendix A. Number Theory

A good introduction to Number Theory is [88]. We introduce a selection of interesting fields and rings with a mind to applications in quantum computation and quantum gravity.

By definition, a *number field* extends the rationals by one special real number α, containing all numbers of the form $a + b\alpha$ for a and b in $\mathbb{Q}$. Multiplication and addition in this field $\mathbb{Q}(\alpha)$ work in the obvious way. Given α, there is a ring of integers in $\mathbb{Q}(\alpha)$, but this is not always the integer multiples of the form $a + b\alpha$. For example, when $\alpha = \sqrt{5}$, the ring of integers consists of numbers $a + b\phi$, where $\phi = (1 + \sqrt{5})/2$ is the golden ratio.

An *algebraic number* is a root of a finite polynomial with rational coefficients, such that the leading coefficient is 1. The golden ratio is algebraic as a root of $X^2 - X - 1 = 0$. Given an algebraic number, there exists a unique such polynomial (of a given degree) with α as a root. It is useful to factorise the polynomial. Consider the quadratic $X^2 - k = (X + \sqrt{k})(X - \sqrt{k}) = 0$ of degree 2. The set of roots $\{+\sqrt{k}, -\sqrt{k}\}$ are called *conjugates* for the field $\mathbb{Q}(\sqrt{k})$, and we use this term for polynomials of any degree d. In terms of the d conjugates, where $\alpha = \alpha_1$, the norm of a number α is defined by

$$N(\alpha) = \prod_{i=1}^{d} \alpha_i. \tag{A.1}$$

Thus $N(\phi) = \phi \cdot (-1/\phi) = -1$, while $X^2 + 3 = 0$ gives $N(\sqrt{-3}) = 3$.

Given a set of conjugates for α, any other element β in $\mathbb{Q}(\alpha)$ may be written in the form

$$\beta = a_0 + a_1\alpha + a_2\alpha^2 + \cdots + a_{d-1}\alpha^{d-1}, \tag{A.2}$$

where the a_i are rational or integer as required. The *field conjugates* of β are the $d-1$ numbers of the form $a_0\alpha_i + \cdots + a_{d-1}\alpha_i^{d-1}$.

Take a basis $\{\beta_1, \beta_2, \cdots, \beta_d\}$ of $\mathbb{Q}(\alpha)$. Typically, we will choose the basis $\{1, \alpha, \alpha^2, \cdots, \alpha^{d-1}\}$. Now for any $\mathbb{Q}(\alpha)$, the basis defines a $d \times d$ matrix M_{ij} with columns indexed by the basis and rows by the conjugates of α. Many examples are given below. The *discriminant* of $\mathbb{Q}(\alpha)$ is defined by the determinant square $\Delta = \mathrm{Det}(M)^2$.

Appendix A.1. Quadratic fields

The degree d is a quantum dimension, since 2×2 matrices ought to be about qubits. When $\alpha = \sqrt{k}$ for an integer k with no square factors, the polynomial $X^2 - k = 0$ defines the field matrix

$$M = \begin{pmatrix} 1 & \sqrt{k} \\ 1 & -\sqrt{k} \end{pmatrix} \tag{A.3}$$

with discriminant $\Delta = 4k$. But for $\sqrt{-3}$, the ring of integers has a basis $\{1, (-1 + \sqrt{-3})/2\}$, so that $\Delta = -3$. Similarly, other negative values of k give negative integral discriminants, in contrast to the positive example of $\mathbb{Q}(\sqrt{5})$, which has $\Delta = 5$ coming from

$$\begin{pmatrix} 1 & \phi \\ 1 & -1/\phi \end{pmatrix}. \tag{A.4}$$

There are no additional field conjugates in the quadratic case. The opposite sign in $N(\phi) = -1$, compared to an ordinary complex norm, is responsible for time in a Lorentzian metric, and $3+5 = 8$ dimensions are associated to the adjoint representation of $SU(3)$ and octonion algebras.

Appendix A.2. Fields on cube roots

Note that the signs in (A.4) give the 2×2 Hadamard matrix. In dimension 3, we see the qutrit 3×3 Fourier transform in the field matrix. Let $\omega = (-1 + \sqrt{-3})/2$ be the cube root of unity above. For the polynomial $X^3 - k = 0$ with k cube free, we have

$$M = \begin{pmatrix} 1 & k^{1/3} & k^{2/3} \\ 1 & \omega k^{1/3} & \overline{\omega} k^{2/3} \\ 1 & \overline{\omega} k^{1/3} & \omega k^{2/3} \end{pmatrix}. \tag{A.5}$$

Hopefully it is clear that 27 is an important number! This is the determinant square of the Fourier transform, and we have in general $\Delta = -27k^2$.

An elliptic curve C of genus 1 takes the standard form $Y^2 = X^3 + aX + b$ for rational coefficients, and has a cubic discriminant $\Delta_C = 4a^3 + 27b^2$, generalising the example above. If a prime p divides Δ_C, then $\Delta_C = 0$ in the finite field $\mathbb{F}_p$. The finite set of $\mathbb{F}_p$ solutions to C defines a Mordell-Weil group for C, whose order $N_p(C)$ appears in the zeta function for C.

Appendix A.3. Fields on fourth roots

When α is a fourth root, we find that $\Delta = -k^3$ for $X^4 - k = 0$. The matrix is

$$\begin{pmatrix} 1 & k^{1/4} & k^{1/2} & k^{3/4} \\ 1 & ik^{1/4} & -k^{1/2} & -ik^{3/4} \\ 1 & -k^{1/4} & k^{1/2} & -k^{3/4} \\ 1 & -ik^{1/4} & -k^{1/2} & ik^{3/4} \end{pmatrix}. \tag{A.6}$$

Let $\rho = \sqrt{\phi + 2}$ be the diagonal of the golden rectangle. It is algebraic because $\rho^4 - 5\rho^2 + 5 = 0$. There are two nice bases for the integers in $\mathbb{Q}(\rho)$, namely

$$\begin{pmatrix} 1 & \rho & \rho^2 & \rho^3 \\ 1 & -\rho & \rho^2 & -\rho^3 \\ 1 & \sqrt{5} & 5 & 5\sqrt{5} \\ 1 & -\sqrt{5} & 5 & -5\sqrt{5} \end{pmatrix} \quad \text{and} \quad \begin{pmatrix} 1 & \rho & \phi & \rho\phi \\ 1 & -\rho & \phi & -\rho\phi \\ 1 & \sqrt{5} & 3 & 3\sqrt{5} \\ 1 & -\sqrt{5} & 3 & -3\sqrt{5} \end{pmatrix}, \tag{A.7}$$

both with $\Delta = 1055.7281$. The second basis forms the *golden ring* of integers of the form

$$x_0 + x_1\phi + x_2\rho + x_3\rho\phi \tag{A.8}$$

for $x_i \in \mathbb{Z}$. Note that $\sqrt{5} = 2\phi - 1$. In the complex field $\mathbb{Q}(\rho, i)$, the ring of integers defines a dense map of $\mathbb{Z}^8$ into $\mathbb{C}$.

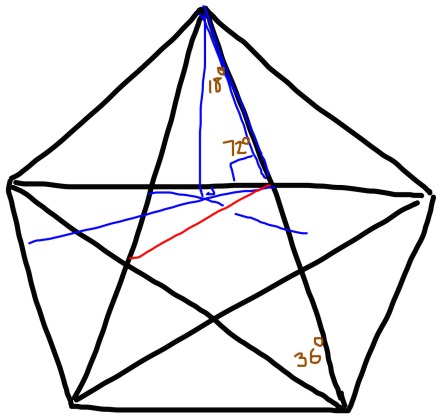

Figure A1. Angle 36° bisection

Figure A1 indicates one of ten possible blue rectangles covering much of the pentagram. The 10 external blue points define a decagon. The chord length on a unit side decagon is ρ.

Appendix A.4. Fields on fifth and higher roots
Using the golden phase $e^{2\pi i/5}$, the discriminant for $X^5 - k = 0$ is $\Delta = 5^5 k^4$. For example, when $k = 4$ we have $\Delta = 800000$. We are interested in prime dimensions d for qudit computation spaces. Let θ be the primitive d-th root of unity. For d prime, the phase coefficients θ^{ij} for $i, j \in \{0, 1, \cdots, d-1\}$ always define the discrete Fourier transform. Δ for $X^p - k = 0$ looks like $p^p k^{p-1}$.

Appendix A.5. Primes and lattices
For quadratic fields, there is a quadratic form that characterises the norm. As expected, the form $f = aX^2 + bXY + cY^2$ comes with the discriminant $\Delta_f = b^2 - 4ac$. In particular, for $\mathbb{Z}[\omega]$ in $\mathbb{Q}(\sqrt{-3})$ we have $\Delta_f = -3$ from $X^2 + XY + Y^2$. For $\mathbb{Z}[\phi]$ the form is $X^2 + XY - Y^2$ and $\Delta_f = 5$. The form $X^2 + Y^2$ matches the Gaussian integers $\mathbb{Z}[i]$. Here $\mathbb{Q}(\sqrt{5})$ requires ϕ because 5 equals +1 mod 4. For positive primes $p \geq 7$ that equal 3 mod 4, such as 7 and 11, the integers have the simple basis $\{1, \sqrt{p}\}$, while $-7 = 1$ mod 4 uses $(-1 + \sqrt{-7})/2$.

The Galois primes $\{2, 3, 5, 7, 11\}$ give the angles for Lie algebra root systems, which satisfy the lattice condition

$$4\cos^2(\frac{2\pi}{p+1}) \in \{0, 1, 2, 3\}. \tag{A.9}$$

Beyond Lie algebras there are other important lattices, notably the Leech lattice in dimension 24 [50].

References

[1] Sheppeard M D 2019 *J. Phys.: Conf. Ser.* **1194** 012097
[2] Sheppeard M D 2017 The algebra of non local neutrino gravity *Preprint* viXra:1712.0076
[3] Street R 2007 *Quantum groups: a path to current algebra* (Cambridge)
[4] Joyal A and Street R 1993 *Adv. Math.* **102** 20
[5] Bakalov B and Kirillov Jr A 2001 *Lectures on tensor categories and modular functors* (New York: A.M.S.)
[6] Wen X G 2020 A systematic construction of gapped non liquid states *Preprint* arXiv:2020.02433
[7] Wang H, Li Y, Hu Y and Wan Y 2020 Electric-magnetic duality in the quantum double models of topological orders with gapped boundaries *J. High E. Phys.* 2 **2020** 030
[8] Huang S J 2020 $4D$ beyond-cohomology topological phase protected *Preprint* arXiv:2001.07772
[9] Cong I, Cheng M and Wang Z 2016 Topological quantum computation with gapped boundaries *Preprint* arXiv:1609.02037
[10] Liu Y, Liu Y and Prodan E 2020 *Ann. Phys.* **414** 168089
[11] Dungworth G 2010 astrophysics posts *Preprint* GalaxyZoo forums
[12] Sheppeard M D 2010 theory posts *Preprint* Arcadian Pseudofunctor
[13] Zhang X T, Gao Y H, Liu C and Chen G 2020 *Phys. Rev. Res.* **2** 013066
[14] Guo H, Samajdar R, Scheurer M S and Sachdev S 2020 *Preprint* arXiv:2002.01947
[15] Witten E 1989 *Commun. Math. Phys.* **121** 351
[16] Maraner P, Pachos J K and Palumbo G 2019 *Sci. Rep.* **9** 17308
[17] Witten E 2014 Two lectures on the Jones polynomial and Khovanov homology *Preprint* arXiv:1401.6996
[18] Witten E 2020 talk presented at Geometry of Quantum Fields and Strings *Preprint* University of Auckland
[19] Jones V F R 1985 *Bull. Amer. Math. Soc.* **12** 103
[20] Khovanov M 2000 *Duke Math. J.* **101** 359
[21] Bar-Natan D and Morrison S 2006 *Algebr. Geom. Topol.* **6** 1459
[22] Dvali G and Funcke L 2016 *Phys. Rev.* D **93** 113002
[23] Funcke L 2018 *How gravity shapes the low energy frontier of particle physics* (Munich: Max Planck Institute)
[24] MacLane S and Moerdijk I 1994 *Sheaves and Geometry in Logic* (Berlin: Springer)
[25] Asselmeyer-Maluga T and Brans C H 2007 *Exotic smoothness and physics* (Singapore: World Scientific)
[26] Yoshida M 1996 *Kyushu J. Math.* **50** 493
[27] Stasheff J D 1963 *Trans. Amer. Math. Soc.* **108** 293
[28] Gukov S, Schwarz A and Vafa C 2005 *Lett. Math. Phys.* **74** 53-74
[29] Beigi S, Shor P W and Whalen D 2010 The quantum double model with boundary: condensations and symmetries *Preprint* arXiv:1006.5479
[30] Battaglia F and Prato E 2010 *Commun. Math. Phys.* **299** 577
[31] Davydov A and Booker T 2011 *J. Alg.* **355** 176
[32] Irwin K, Amaral M M, Aschheim R and Fang F 2016 *Proc. 4th International Conf. on the Nature and Ontology of Spacetime (Varna)* (Minkowski Institute) p 117
[33] Freedman M 1982 *J. Diff. Geom.* **17** 357
[34] Eguchi T, Ooguri H, Taormina A and Yang S K 1989 *Nucl. Phys.* B **315** 193
[35] Eguchi T, Ooguri H and Tachikawa Y 2011 *Exper. Math.* **20** 91
[36] Gannon T 2016 *Adv. Math.* **301** 322
[37] Cheng M C N, Duncan J F R and Harvey J A 2014 *Res. Math. Sci.* **1** 3
[38] Furey C 2012 *Phys. Rev.* D **86** 025024
[39] Furey C 2015 *Phys. Lett.* B **742** 195
[40] Barenz M and Barrett J 2018 *Commun. Math. Phys.* **360** 663
[41] Kirby R C 1978 *Invent. Math.* **45** 35
[42] Qi X L, Li R, Zang J and Zhang S C 2009 *Science* **323** 1184
[43] Crane L and Sheppeard M D 2003 Poincare representations and state sums *Preprint* arXiv:math.QA/0306440
[44] Witten E 2007 Three dimensional gravity revisited *Preprint* arXiv:0706.3359
[45] Sheppeard M D 2019 Discrete motives for moonshine *Preprint* viXra:1906.0443
[46] Rios M 2018 private communication
[47] Elgueta J 2002 *Cohomology and Theory of Deformations of semigroupal* 2*-categories* (Polytechnic University of Catalonia)
[48] Baez J C 1997 *Preprint* math.ucr.edu/baez/week102.html
[49] Wilson R A 2009 *J. Alg.* **322** 2186

[50] Wilson R A 2009 *The finite simple groups* (Berlin: Springer)
[51] Cannon J W, Floyd W J and Parry W R 1996 *Enseign. Math.* **2** 215
[52] Inoue Y 2016 The four color theorem and Thompson's F and links *Preprint* http://math.nsc.ru/conference/g2/g2s2/exptext/inoue.pdf
[53] Heinze A and Klin M 2009 *Loops, Latin squares and strongly regular graphs* (Algorithmic algebraic combinatorics and Grobner bases) ed M. Klin (Berlin: Springer) chapter 1
[54] Schwinger J 1960 *Proc. Nat. Acad. Sci. USA* **46** 570
[55] Wootters W K and Fields B D 1989 *Ann. Phys.* **191** 363
[56] Combescure M 2009 *J. Math. Phys.* **50** 032104
[57] Ng S H, Schopieray A and Wang Y 2019 *Selecta Math.* **25** 53
[58] Duncan R and Dunne K 2016 Interacting Frobenius algebras are Hopf *Preprint* arXiv:1601.04964
[59] Koide Y 1983 *Phys. Rev.* D **28** 252
[60] Koide Y 1983 *Phys. Lett.* B **120** 161
[61] Brannen C A 2006 The lepton masses *Preprint* http://www.brannenworks.com
[62] Sheppeard M D 2017 Neutrino mixing with Hopf algebras *Preprint* viXra:1709.0035
[63] Johnstone P T 1982 *Stone spaces* (Cambridge)
[64] Abramsky S and Coecke B 2004 A categorical semantics of quantum protocols *Proc. of the 19th Annual Symp. on Logic in Computer Science* (IEEE) p 415
[65] Sheppeard M D 2007 *Gluon phenomenology and a linear topos* (Christchurch: University of Canterbury)
[66] Truini P, Rios M and Marrani A 2017 The magic star of exceptional periodicity *Preprint* arXiv:1711.07881
[67] Coecke B, Pavlovic D and Vicary J 2013 *Math. Structures in Comp. Sci.* **23** 555
[68] Chisholm E L and McCammond J 2015 Braid groups and Euclidean simplices *Configuration Spaces* (Berlin: Springer) p 291
[69] McCammond J and Sulway R 2017 Artin groups of Euclidean type *Preprint* http://web.math.ucsb.edu/ mccammon/papers/artin-euclid-revised.pdf
[70] Kauffman L H 2018 *Int. J. Mod. Phys.* A **33** 1830023
[71] Kauffman L H and Lomonaco Jr S L 2008 The Fibonacci model and the Temperley-Lieb algebra *Preprint* arXiv:0804.4304
[72] Siehler J 2003 *Alg. Geom. Top.* **3** 719
[73] Cui S X, Zini M S and Wang Z 2019 *Science China Math.* **62** 417-446
[74] Hu Y, Wan Y and Wu Y S 2013 Twisted quantum double model of topological phases in two dimensions *Preprint* arXiv:1211.3695
[75] Itzykson C 1994 *Topics in conformal field theory* (ANU Summer School: Statistical mechanics and field theory) ed V. V. Bazhanov (Singapore: World Scientific) p 168
[76] Gine J 2012 *Mod. Phys.* A **27** 1250208
[77] McCulloch M E and Gine J 2017 *Mod. Phys.* A **32** 1750148
[78] L. Riofrio, http://riofriospacetime.blogspot.com
[79] Ghrist R W 1995 *Elec. Res. Announc. A.M.S.* **1** 91
[80] Kauffman L H, Saito M and Sullivan M C 2003 *J. Knot Th. Ram.* **12** 653
[81] Field B and Simula T 2018 *Quantum Sci. and Tech.* **3** 4
[82] Bilson-Thompson S O 2005 A topological particle spectrum *Preprint* arXiv:hep-ph/0503213
[83] Postnikov A 2009 *Int. Math. Res. Not.* **2009** 1026
[84] Richter D 2012 How to make $M24$ *Preprint* http://homepages.wmich.edu/ drichter/mathieu.htm
[85] Lack S 2004 *Theory Applic. Cat.* **13** 147
[86] MacLane S 2000 *Categories for the working mathematician* (New York: Springer)
[87] Virelizier A 2010 *Quantum invariants of 3-manifolds, TQFTs and Hopf monads* (University of Montpellier 2)
[88] Rose H R 1994 *A course in Number Theory* (Oxford)